CLNS 06/1970
CLEO 06-15

Improved Measurement of the Branching Fraction and Energy Spectrum of η' from $\Upsilon(1S)$ Decays

O. Aquines, Z. Li, A. Lopez, S. Mehrabyan, H. Mendez, and J. Ramirez
University of Puerto Rico, Mayaguez, Puerto Rico 00681

G. S. Huang, D. H. Miller, V. Pavlunin, B. Sanghi, I. P. J. Shipsey, and B. Xin
Purdue University, West Lafayette, Indiana 47907

G. S. Adams, M. Anderson, J. P. Cummings, I. Danko, and J. Napolitano
Rensselaer Polytechnic Institute, Troy, New York 12180

Q. He, J. Insler, H. Muramatsu, C. S. Park, E. H. Thorndike, and F. Yang
University of Rochester, Rochester, New York 14627

T. E. Coan, Y. S. Gao, and F. Liu
Southern Methodist University, Dallas, Texas 75275

M. Artuso, S. Blusk, J. Butt, J. Li, N. Menaa, R. Mountain, S. Nisar, K. Randrianarivony, R. Redjimi, R. Sia, T. Skwarnicki, S. Stone, J. C. Wang, and K. Zhang
Syracuse University, Syracuse, New York 13244

S. E. Csorna
Vanderbilt University, Nashville, Tennessee 37235

G. Bonvicini, D. Cinabro, M. Dubrovin, and A. Lincoln
Wayne State University, Detroit, Michigan 48202

D. M. Asner and K. W. Edwards
Carleton University, Ottawa, Ontario, Canada K1S 5B6

R. A. Briere, I. Brock, J. Chen, T. Ferguson, G. Tatishvili, H. Vogel, and M. E. Watkins
Carnegie Mellon University, Pittsburgh, Pennsylvania 15213

J. L. Rosner

Enrico Fermi Institute, University of Chicago, Chicago, Illinois 60637

N. E. Adam, J. P. Alexander, K. Berkelman, D. G. Cassel, J. E. Duboscq, K. M. Ecklund, R. Ehrlich, L. Fields, R. S. Galik, L. Gibbons, R. Gray, S. W. Gray, D. L. Hartill, B. K. Heltsley, D. Hertz, C. D. Jones, J. Kandaswamy, D. L. Kreinick, V. E. Kuznetsov, H. Mahlke-Krüger, P. U. E. Onyisi, J. R. Patterson, D. Peterson, J. Pivarski, D. Riley, A. Ryd, A. J. Sadoff, H. Schwarthoff, X. Shi, S. Stroiney, W. M. Sun, T. Wilksen, and M. Weinberger

Cornell University, Ithaca, New York 14853

S. B. Athar, R. Patel, V. Potlia, and J. Yelton

University of Florida, Gainesville, Florida 32611

P. Rubin

George Mason University, Fairfax, Virginia 22030

C. Cawlfield, B. I. Eisenstein, I. Karliner, D. Kim, N. Lowrey, P. Naik, C. Sedlack, M. Selen, E. J. White, and J. Wiss

University of Illinois, Urbana-Champaign, Illinois 61801

M. R. Shepherd

Indiana University, Bloomington, Indiana 47405

D. Besson

University of Kansas, Lawrence, Kansas 66045

T. K. Pedlar

Luther College, Decorah, Iowa 52101

D. Cronin-Hennessy, K. Y. Gao, D. T. Gong, J. Hietala, Y. Kubota, T. Klein, B. W. Lang, R. Poling, A. W. Scott, A. Smith, and P. Zweber

University of Minnesota, Minneapolis, Minnesota 55455

S. Dobbs, Z. Metreveli, K. K. Seth, and A. Tomaradze

Northwestern University, Evanston, Illinois 60208

J. Ernst

State University of New York at Albany, Albany, New York 12222

H. Severini

University of Oklahoma, Norman, Oklahoma 73019

S. A. Dytman, W. Love, and V. Savinov

University of Pittsburgh, Pittsburgh, Pennsylvania 15260

(Dated: October 10, 2006)

Abstract

We present an improved measurement of the η' meson energy spectrum in $\Upsilon(1S)$ decays, using 1.2 fb^{-1} of data taken at the $\Upsilon(1S)$ center-of-mass energy with the CLEO III detector. We compare our results with models of the η' gluonic form factor that have been suggested to explain the unexpectedly large $B \to \eta' X_s$ rate. Models based on perturbative QCD fail to fit the data for large η' energies, and thus an explanation outside the realm of the Standard Model or an improved understanding of non-perturbative QCD effects may be needed to account for this large rate.

PACS numbers: 13.25.Gv,13.25.Hw,13.66.Bc

I. INTRODUCTION

CLEO observed a surprisingly large branching fraction for the decay $B \to \eta' X_s$ at large momenta of the η' meson $p_{\eta'}$: $\mathcal{B}(B \to \eta' X_s)|_{p_{\eta'}>2\ GeV} = (6.2 \pm 1.6 \pm 1.3^{+0.0}_{-1.5}) \times 10^{-4}$ [1, 2]. BaBar [3] later obtained $\mathcal{B}(B \to \eta' X_s)|_{p_{\eta'}>2\ GeV} = (3.9 \pm 0.8 \pm 0.5 \pm 0.8) \times 10^{-4}$. This η' momentum is beyond the end point for most $b \to c$ decays, so the η' yield from $b \to c$ is expected to be only of the order of 1×10^{-4}. Predictions assuming factorization [4, 5] estimate the charmless component of this branching fraction to be also about 1×10^{-4}. Thus conventional calculations cannot account for the measured rate and they also fail to predict the right shape for the η' momentum spectrum [6]. These findings motivated intense theoretical activity because new physics could account for such an enhancement. However, Standard Model explanations have also been proposed. For example, Atwood and Soni [7] argued that the observed excess is due to an enhanced $b \to sg$ penguin diagram, complemented by a strong $\eta' g g^\star$ coupling, induced by the gluonic content of the η' wave function. Fig. 1 (left) shows the corresponding Feynman diagram. The high q^2 region of the $g^\star g \eta'$ vertex function involved in this process also affects fast η' production in $\Upsilon(1S)$ decay [6–8], whose relevant diagram is shown in Fig. 1 (right). Thus a precise measurement of the η' inclusive spectra from the process $\Upsilon(1S) \to ggg^\star \to \eta' X$ can improve our understanding of important B meson decays.

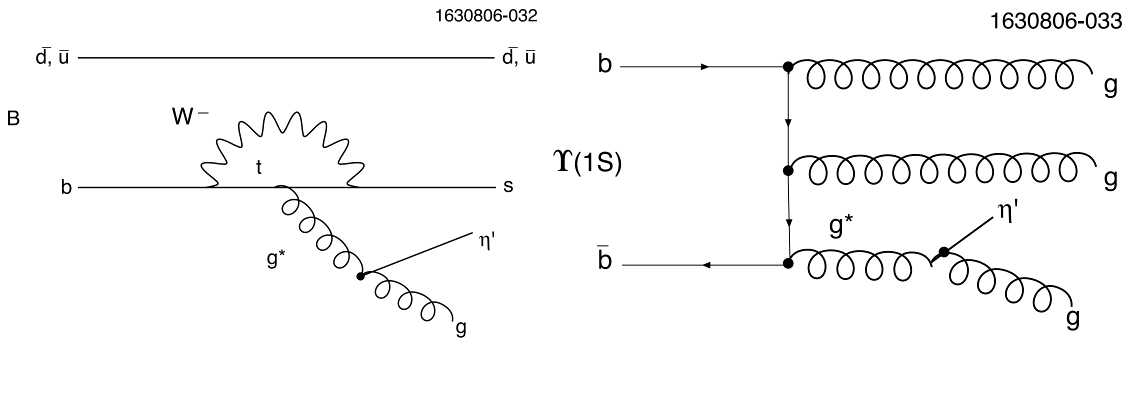

FIG. 1: Feynman Diagram for $b \to s(g^\star \to g\eta')$ (left) and $\Upsilon(1S) \to ggg^\star \to \eta' X$ (right).

The effective vertex function $\eta' g g^\star$ can be written as [7] $H(q^2)\delta^{ab}\varepsilon_{\alpha\beta\mu\nu}q^\alpha k^\beta \varepsilon_1^\mu \varepsilon_2^\nu$, where q is the $(g^\star)$ virtual gluon's four-momentum, k is the (g) "on-shell" gluon's momentum ($k^2 = 0$), a, b represent color indices, $\varepsilon_1^\mu, \varepsilon_2^\nu$ are the polarization vectors of the two gluons, and $H(q^2)$ is the $g^\star g \eta'$ transition form factor. Different assumptions on the form factor dependence have been proposed [5, 7–11].

While ARGUS was the first experiment to study the inclusive η' production at the $\Upsilon(1S)$ [12], they did not have enough data to separate $\Upsilon(1S) \to ggg^\star$ from the other components discussed below. CLEO II [13] was the first experiment to have sufficient statistics to measure inclusive η' production from the subprocess $\Upsilon(1S) \to ggg^\star$. These data ruled out a class of form factors characterized by a very weak q^2 dependence [7, 9]. Subsequently, several theoretical calculations [8, 10, 11] derived the perturbative QCD form factors from models of the η' wave function. Attempts to use CLEO II data to constrain the model parameters [14] were not conclusive, due to the limited statistics at the end point of the η' spectrum. Thus, it was difficult to establish whether neglecting higher order terms in the perturbative expansion was appropriate [14]. An improved measurement, based on a higher-statistics sample, is important to provide an improved determination of the QCD parameters, and, consequently, a more stringent test of the theory. This work reports a new measurement of the inclusive η' spectrum from the process $\Upsilon(1S) \to ggg^\star \to \eta' X$ based on the largest $\Upsilon(1S)$ sample presently available, more than a factor of 11 greater than the previous study [13].

II. DATA SAMPLE AND ANALYSIS METHOD

We use 1.2 fb^{-1} of CLEO III data recorded at the $\Upsilon(1S)$ resonance, at 9.46 GeV center-of-mass energy, containing 21.2×10^6 events, and off-resonance continuum data collected at center-of-mass energies of 10.54 GeV (2.3 fb^{-1}).

The CLEO III detector includes a high-resolution charged particle tracking system [15], a CsI electromagnetic calorimeter [16], and a Ring Imaging Cherenkov (RICH) hadron identification system [17]. The CsI calorimeter measures the photon energies with a resolution of 2.2% at $E = 1$ GeV and 5% at E=100 MeV. The tracking system also provides charged particle discrimination, through the measurement of the specific ionization dE/dx.

We detect η' mesons through the channel $\eta' \to \eta\pi^+\pi^-$, with $\eta \to \gamma\gamma$. The branching fractions for these processes are (44.5$\pm$1.4)% and (39.38$\pm$0.26)% [19] respectively. We identify single photons based on their shower shape. The photon four-vectors are constrained to have invariant mass equal to the nominal η mass. Subsequently, η candidates are combined with two oppositely charged tracks to form an η'. Loose π consistency criteria based on

dE/dx measurements are applied to the charged tracks.

The gluonic η' production at the $\Upsilon(1S)$ is expected to be dominant only at very high q^2, or, equivalently, at high η' scaled energy Z, where Z is defined as

$$Z \equiv \frac{E_{\eta'}}{E_{\rm beam}} = \frac{2E_{\eta'}}{M_{\Upsilon(1S)}}, \tag{1}$$

where $E_{\eta'}$ is the η' energy and $E_{\rm beam}$ is the beam energy. Enhanced η' production at high Z would indicate a large $\eta' g^\star g$ coupling.

For low-energy η' mesons, photons coming from low energy π^0s are a severe source of background. Thus a π^0 veto is applied for $Z < 0.5$, whereby photon pairs that have an invariant mass consistent within 2.5 σ with the nominal π^0 mass are not included as the candidate photons for η reconstruction. We consider only η' with scaled energy Z between 0.2 and 1 and divide this range into eight equal bins. Fig. 2 shows the η' yields in these bins for the $\Upsilon(1S)$ sample. Fig. 3 shows the corresponding distributions from the continuum sample taken at a center-of-mass energy of 10.54 GeV. In order to derive the η' signal yields, we fit the $\Delta M_{\eta'\eta}$ distributions $[\Delta M_{\eta'\eta} \equiv M(\pi^+\pi^-\eta) - M(\eta)]$ in each Z bin with a Gaussian function representing the signal, and a polynomial background. The Gaussian is used only to define a $\pm 2.5\sigma$ signal interval. Then the η' yield in this interval is evaluated counting events in the signal window, after subtracting the background estimate obtained from the fit function. As the $\Delta M_{\eta'\eta}$ signal is not described well by a single Gaussian function, this procedure minimizes systematic uncertainties associated with the choice of an alternative signal shape.

Information on the gluon coupling of the η' can be drawn only from the decay chain $\Upsilon(1S) \to ggg^\star \to \eta' X$, described by the Feynman diagram in Figure 1. Thus we need to subtract both continuum η' production and η' from the process $\Upsilon(1S) \to \gamma^\star \to q\bar{q}$. The latter component is estimated using

$$\mathcal{B}(\Upsilon(1S) \to q\bar{q}) = R \cdot \mathcal{B}(\Upsilon(1S) \to \mu^+\mu^-) = (8.83 \pm 0.25)\%, \tag{2}$$

where R is the ratio between the hadronic cross section $\gamma^\star \to q\bar{q}$ and the di-muon cross section $\gamma^\star \to \mu^+\mu^-$ at an energy close to 9.46 GeV. We use $R = 3.56 \pm 0.07$ [18] and $\mathcal{B}(\Upsilon(1S) \to \mu^+\mu^-) = (2.48 \pm 0.05)\%$ [19]. The yield $N(\Upsilon(1S) \to ggg^\star)$ is estimated with the relationship

$$N(\Upsilon(1S) \to ggg^\star) = N_{\rm had} - N(\gamma^\star \to q\bar{q}) - N(\Upsilon(1S) \to q\bar{q}), \tag{3}$$

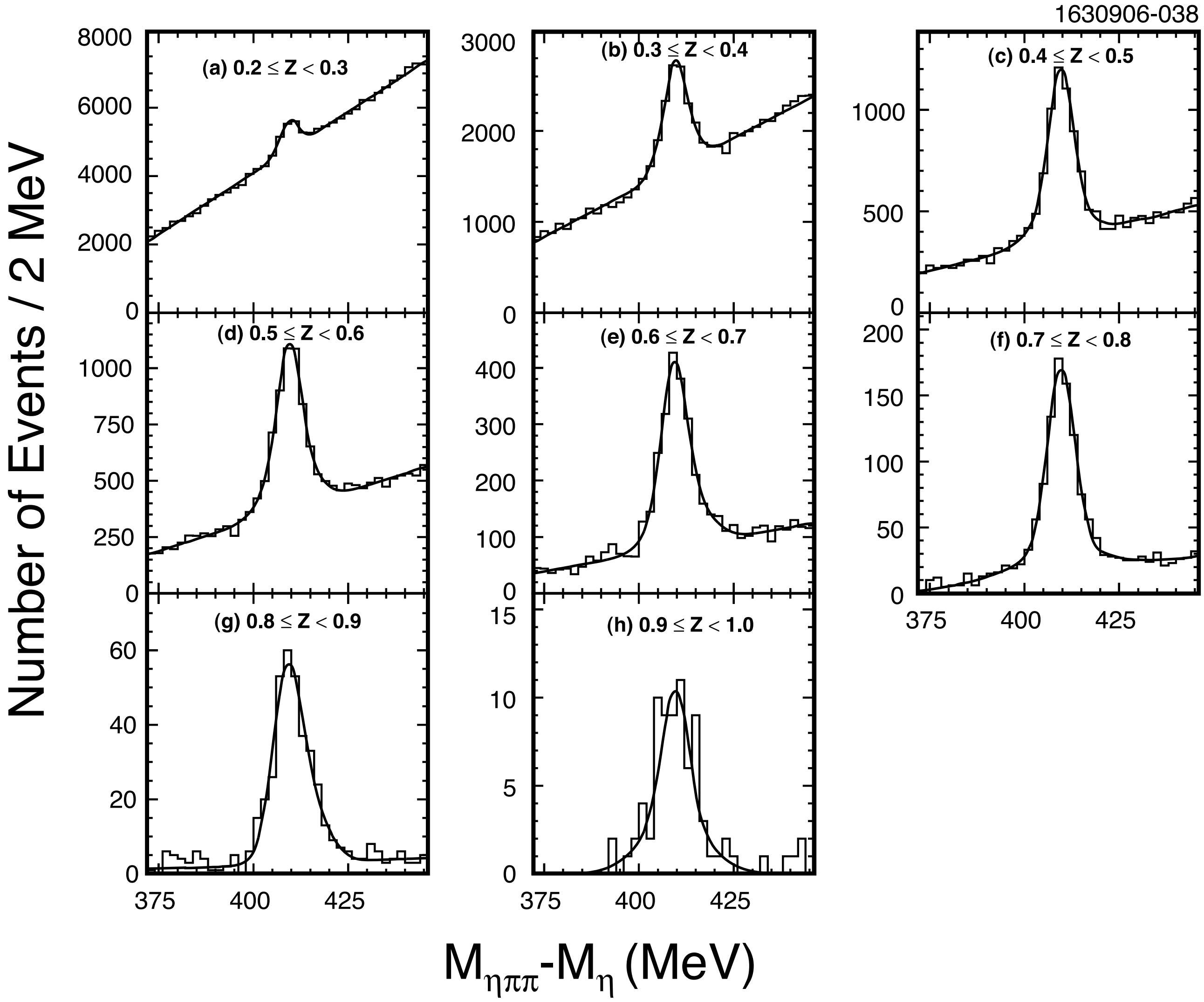

FIG. 2: The spectra of the difference of the $\eta\pi^+\pi^-$ and η invariant masses in different Z ranges reconstructed from $\Upsilon(1S)$ data, fit with a single Gaussian function for the signal and a first-order polynomial for the background.

where $N_{\rm had}$ is the number of hadronic events in our sample, and $N(\gamma^\star \to q\bar{q})$ is the number of continuum events derived from the 10.54 GeV continuum data set, corrected for the luminosity difference between resonance and continuum data, and the center-of-mass dependence of the cross section for the process $\gamma^\star \to q\bar{q}$.

The two dominant components of the η' spectrum have different topologies: $\Upsilon(1S) \to ggg^\star$ produces a spherical event topology, whereas $q\bar{q}$ processes are more jet-like. This difference affects the corresponding reconstruction efficiencies. The γgg cross section is only about 3% of the $ggg^\star$ cross section; thus we make no attempt to subtract the former

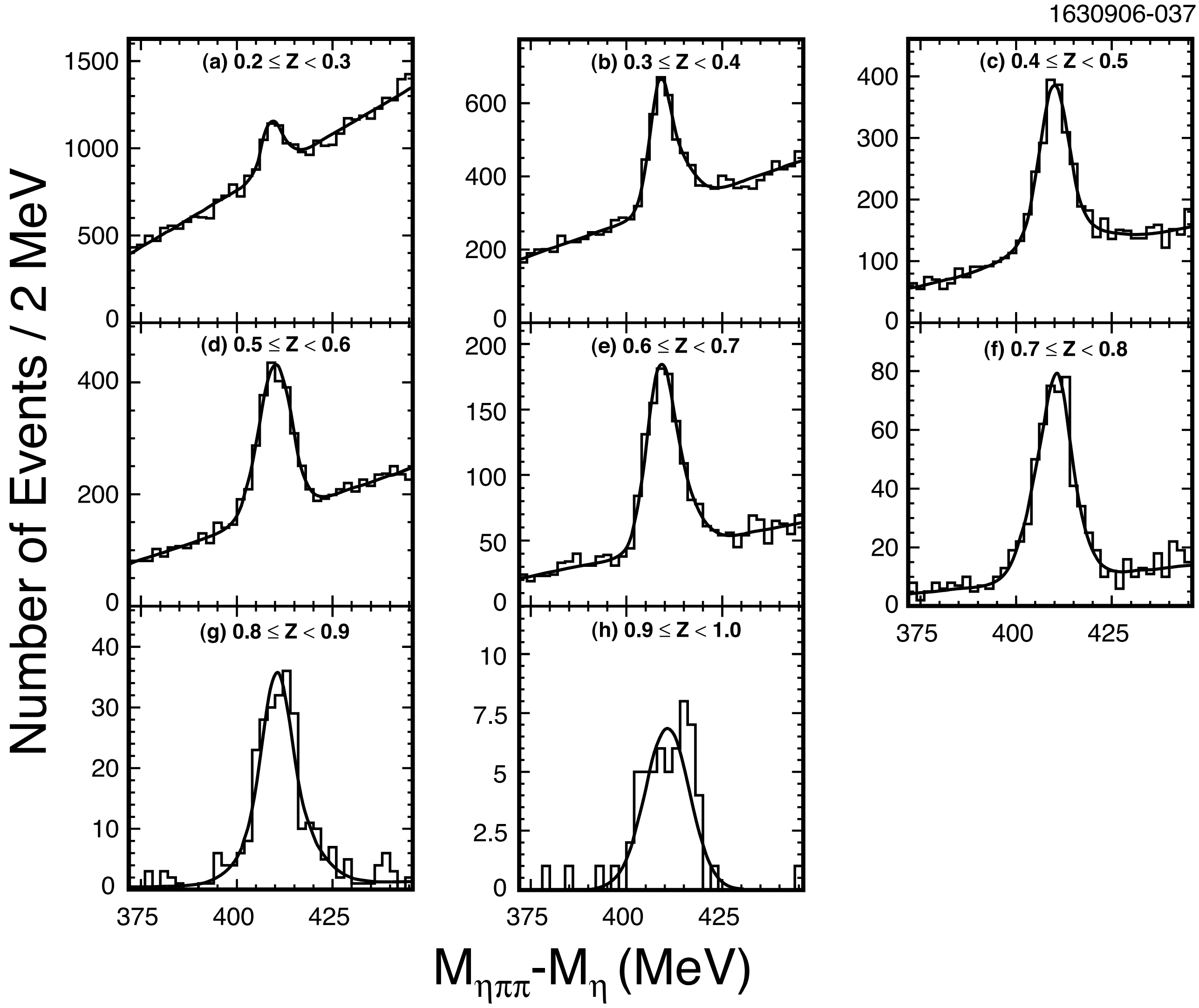

FIG. 3: The spectra of the difference of the $\eta\pi^+\pi^-$ and η invariant masses in different Z ranges reconstructed from continuum data taken at a center-of-mass energy of 10.54 GeV, fit with a single Gaussian function for the signal and a first order polynomial for the background.

component from the latter. Fig. 4 shows the efficiencies obtained for the two event topologies with CLEO III Monte Carlo studies. We use GEANT-based [20] Monte Carlo samples, including $\Upsilon(1S)$ and continuum samples. In order to use the continuum sample taken at 10.54 GeV center-of-mass energy for background subtraction, we develop a "mapping function" to correct for the difference in phase space and Z range spanned in the two samples. The procedure is described in detail in Ref. [13]. In brief, we use the η' energy distribution functions for the Monte Carlo continuum samples at center-of-mass energies equal to 9.46 and 10.54 GeV and obtain a relationship between the measured Z at higher center-of-mass energy $Z_{10.54}$:

$$Z_{9.46} = -0.215\times 10^{-2} + 1.2238\ Z_{10.54} - 0.6879\ (Z_{10.54})^2 + 0.8277\ (Z_{10.54})^3 - 0.3606\ (Z_{10.54})^4\ . \tag{4}$$

We derive the η' spectrum from the decay $\Upsilon(1S) \to ggg^\star \to \eta' X$ from the efficiency corrected η' yields in each Z bin, subtracting the contributions from continuum and $\Upsilon(1S) \to q\bar{q}$ as shown in Equation 3. In this case, the η' spectrum from the process $\Upsilon(1S) \to q\bar{q} \to \eta' X$ is corrected for the distortion introduced by initial state radiation (ISR) on the continuum η' energy spectrum used to account for this effect. The partial yield $N(\Upsilon(1S) \to q\bar{q})(Z)$ is estimated with the relationship

$$\begin{aligned} N(\Upsilon(1S) \to q\bar{q})(Z) &= N(\gamma^\star \to q\bar{q} \to \eta' X)(Z) \times R_{\mathrm{ISR}} \times \frac{\sigma_{\Upsilon(1S)\to q\bar{q}}}{\sigma_{e^+e^-\to q\bar{q}}} \\ &= N(\gamma^\star \to q\bar{q} \to \eta' X)(Z) \times R_{\mathrm{ISR}} \times \frac{\sigma_{\Upsilon(1S)\to \mu^+\mu^-}}{\sigma_{e^+e^-\to \mu^+\mu^-}}, \end{aligned} \tag{5}$$

where R_{ISR} accounts for the difference between the $\Upsilon(1S) \to q\bar{q} \to \eta' X$ and the $\gamma^\star \to q\bar{q} \to \eta' X$ spectra due to initial state radiation (ISR) effects, estimated using Monte Carlo continuum samples with and without ISR simulation, and $\sigma(\Upsilon(1S) \to q\bar{q})/\sigma(e^+e^- \to q\bar{q})$ accounts for the relative cross section of these two processes. The correction factor R_{ISR} differs from 1 by a few percent at low Z and as much as 25% at the end point of the η' energy. The cross sections used are $\sigma(\Upsilon(1S) \to \mu^+\mu^-) = 0.502 \pm 0.010$ nb [19] and $\sigma(e^+e^- \to \mu^+\mu^-) = 1.372 \pm 0.014$ nb [21]. Fig. 5 shows the measured differential cross sections $d\sigma_{\eta'}/dZ$ for the processes $\Upsilon(1S) \to ggg^\star$, $\Upsilon(1S) \to q\bar{q}$, and, $\gamma^\star \to q\bar{q}$.

Theoretical predictions give the energy distribution function $dn/dZ \equiv [1/N(\Upsilon(1S) \to ggg^\star)] \times dN(\Upsilon(1S) \to ggg^\star \to \eta' X)/dZ$; we obtain the corresponding experimental quantity by dividing by the total number of $N(\Upsilon(1S) \to ggg^\star)$, estimated by applying Equation 3 without any Z restriction. Figure 6.a) shows the $\Upsilon(1S) \to ggg^\star \to \eta' X$ energy distribution function, whereas Fig. 6.b) and c) show the corresponding distributions for $\Upsilon(1S) \to q\bar{q} \to \eta' X$, normalized with respect of the total number of $\Upsilon(1S) \to q\bar{q}$ and $\Upsilon(1S) \to \eta' X$, normalized with respect to the total number of $\Upsilon(1S)$.

The inclusive η' production at the $\Upsilon(1S)$ is expected to be dominated by the transition $\Upsilon(1S) \to ggg^\star \to \eta' X$ only at high η' energy. The energy at which this occurs cannot be predicted from first principles: an empirical criterion is the χ^2 of the theory fit to the

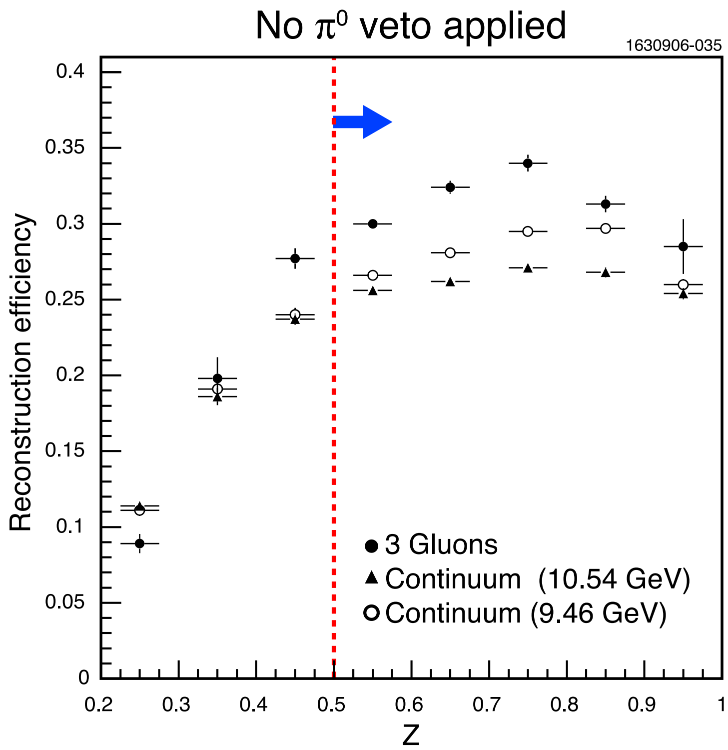

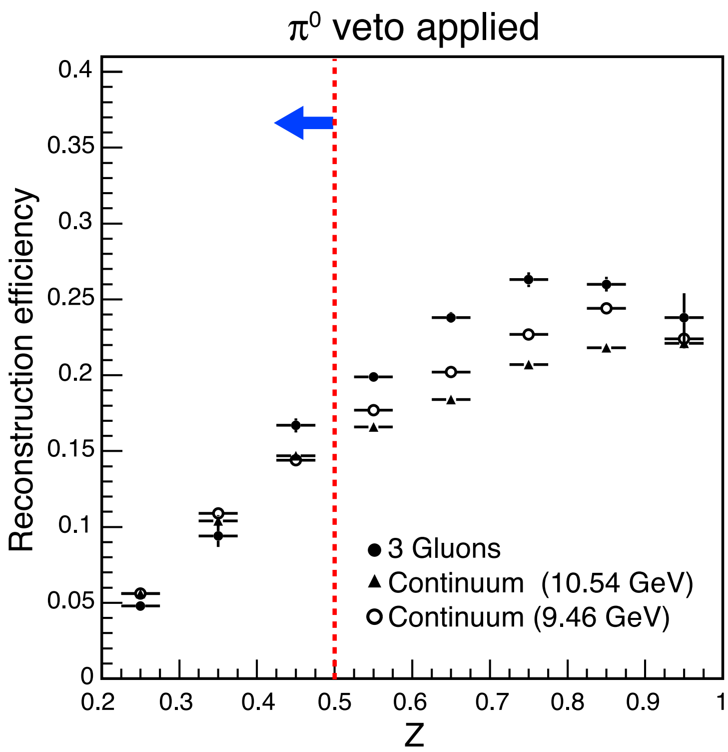

FIG. 4: The η' reconstruction efficiencies as function of Z for different MC samples with no π^0 veto, and with π^0 veto in photon selection. The π^0 veto was applied in this analysis for $Z < 0.5$.

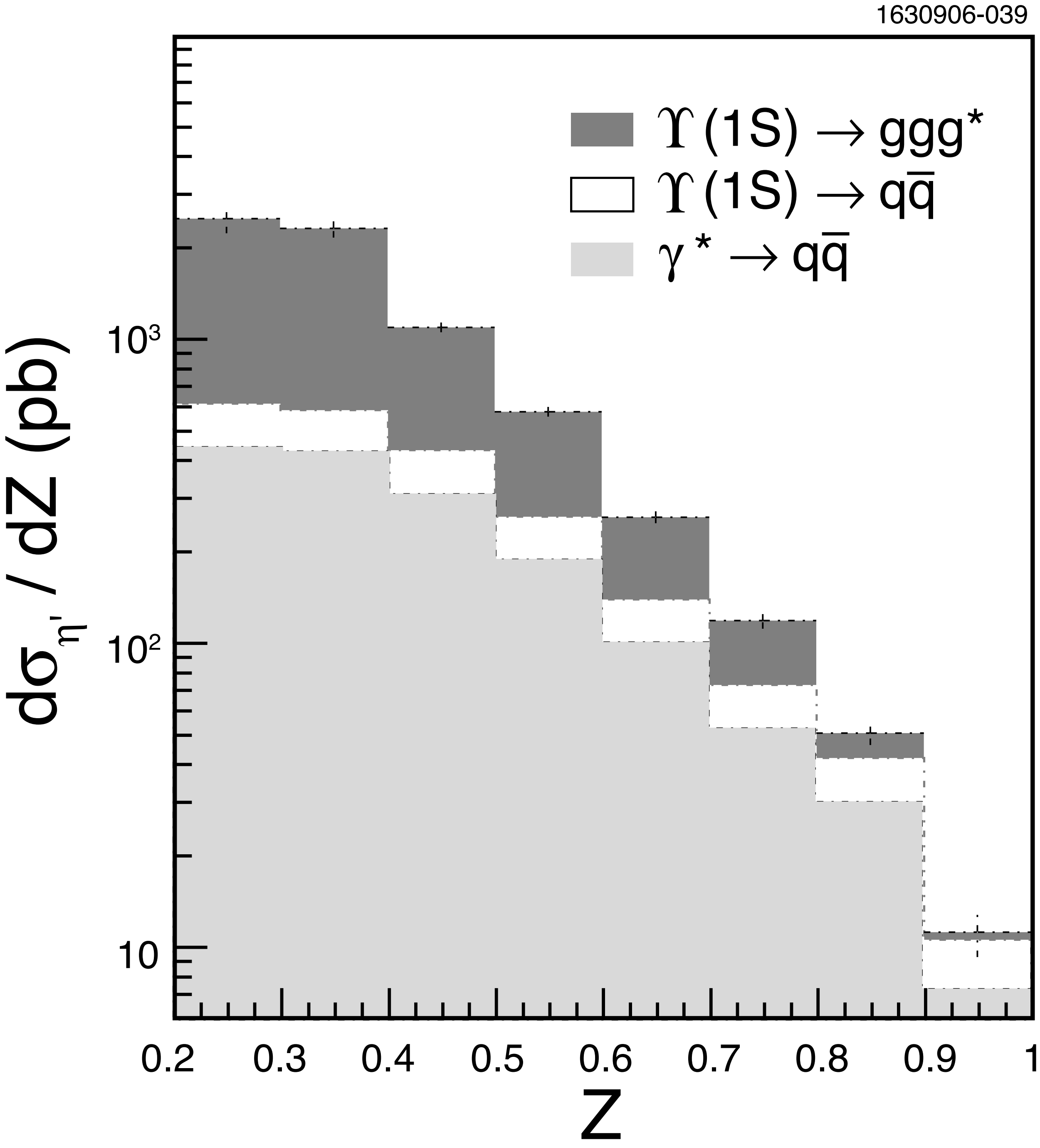

FIG. 5: The measured differential cross sections $d\sigma_{\eta'}/dZ$ for a) $\gamma^\star \to q\bar{q} \to \eta' X$ (shaded), b) $\Upsilon(1S) \to q\bar{q} \to \eta' X$ (white) and c) $\Upsilon(1S) \to ggg^\star \to \eta' X$ (black).

data. For example, a numerical analysis of the CLEO II data [14] obtained a χ^2 of 2.4 for three degrees of freedom, using the 3 experimental points at $Z \geq 0.7$, and ≈ 24 for 4 degrees of freedom using the 4 points at $Z \geq 0.6$. This observation led Ali and Parkhomenko

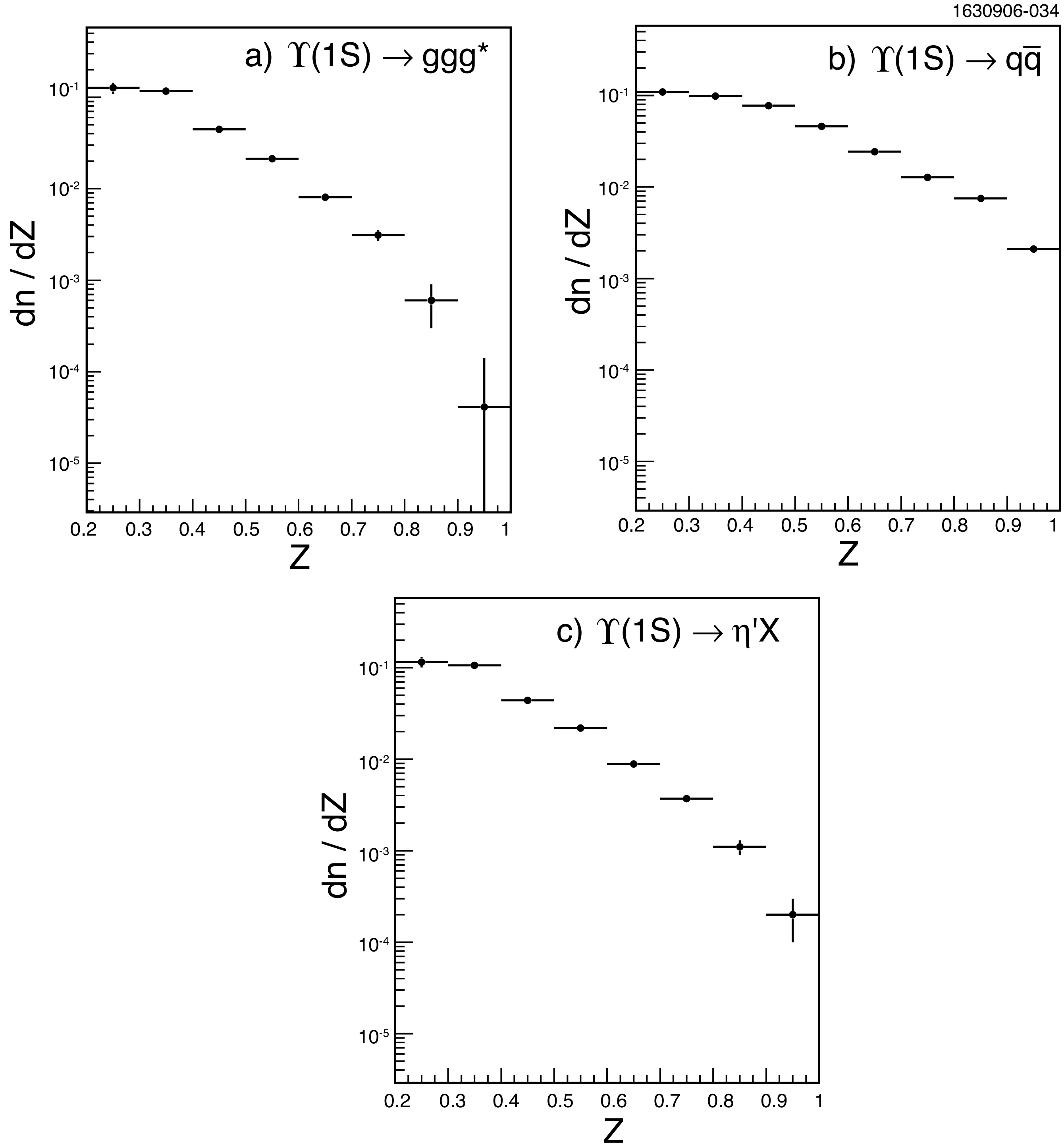

FIG. 6: The energy distribution function dn/dZ as defined in the text for a) $\Upsilon(1S) \to ggg^\star \to \eta' X$, b) $\Upsilon(1S) \to q\bar{q} \to \eta' X$, and c) $\Upsilon(1S) \to \eta' X$.

to conclude that the Z region likely to be dominated by $\Upsilon(1S) \to ggg^\star \to \eta' X$ starts at $Z = 0.7$. Thus we quote global branching fractions for $\Upsilon(1S) \to \eta' X$ and the corresponding results for $Z \geq 0.7$ separately.

Table I summarizes the dominant components of the systematic uncertainties. The overall relative errors on the η' branching fractions are $\pm 8.1\%$ for $q\bar{q} \to \eta' X$, $\pm 9.1\%$ for $ggg^\star \to \eta' X$ for $Z > 0.7$ and $\pm 7.2\%$ for all other branching fractions.

Sources	$ggg^\star$ Sample ($Z > 0.7$)	$q\bar{q}$ Sample	All others
Reconstruction efficiency of $\pi^\pm$	2.0	2.0	2.0
Reconstruction efficiency of η	5.0	5.0	5.0
Number of η' from fit	1.0	1.0	1.0
Total number of $\Upsilon(1S)$	1.0	1.0	1.0
$\mathcal{B}(\eta' \to \pi^+\pi^-\eta)$	3.4	3.4	3.4
$\mathcal{B}(\Upsilon(1S) \to q\bar{q})$	-	3.0	-
Ratio of integrated luminosity	1.9	1.0	-
$\sigma_{\Upsilon(1S)\to\mu^+\mu^-}, \sigma_{e^+e^-\to\mu^+\mu^-}$	0.7	1.3	-
π^0 veto	-	1.7	0.4
Z mapping	6.0	3.0	3.0
Total	9.1	8.1	7.2

TABLE I: The components of the systematic errors (%) affecting the branching fractions reported in this paper.

Thus we obtain

$$\begin{aligned} n(\Upsilon(1S) \to (ggg^\star) \to \eta' X) \equiv \frac{N(\Upsilon(1S) \to ggg^\star \to \eta' X)}{N(\Upsilon(1S) \to ggg^\star)} &= (3.2 \pm 0.2 \pm 0.2)\%, \\ n(\Upsilon(1S) \to (q\bar{q}) \to \eta' X) \equiv \frac{N(\Upsilon(1S) \to q\bar{q} \to \eta' X)}{N(\Upsilon(1S) \to q\bar{q})} &= (3.8 \pm 0.2 \pm 0.3)\%, \\ n(\Upsilon(1S) \to \eta' X) \equiv \frac{N(\Upsilon(1S) \to \eta' X)}{N(\Upsilon(1S))} &= (3.0 \pm 0.2 \pm 0.2)\%. \end{aligned} \quad (6)$$

The $\Upsilon(1S) \to \eta' X$ branching fractions at high momentum (Z > 0.7) are measured to be

$$\begin{aligned} n(\Upsilon(1S) \to (ggg^\star) \to \eta' X)_{Z>0.7} &= (3.7 \pm 0.5 \pm 0.3) \times 10^{-4}, \\ n(\Upsilon(1S) \to (q\bar{q}) \to \eta' X)_{Z>0.7} &= (22.5 \pm 1.2 \pm 1.8) \times 10^{-4}, \\ n(\Upsilon(1S) \to \eta' X)_{Z>0.7} &= (5.1 \pm 0.4 \pm 0.4) \times 10^{-4}. \end{aligned} \quad (7)$$

III. COMPARISON WITH THEORY AND CONCLUSIONS

A. Kagan [6] used the ratio $R_{Z>0.7}$, defined as

$$R_{Z>0.7} \equiv \left[\frac{n_{\rm th}}{n_{\rm exp}}\right]_{Z>0.7}, \tag{8}$$

to obtain a first rough discrimination between form factors having drastically different q^2 dependence. At the time that Ref. [6] was published, the comparison was based on 90% C.L. upper limits on the data. This test repeated with our present data give values of $R_{Z>0.7} \gtrsim 74$ for a representative slowly falling form factor [9], $R_{Z>0.7} \gtrsim 25$ for the intermediate form factor studied by Ref. [5], and $R_{Z>0.7} \gtrsim 2$ for the perturbative QCD inspired shape. Thus the last shape is the closest to the data, but it does not match them very well.

Several perturbative QCD calculations of this process exist, and are based on different choices of the form factor $H(q^2)$: Kagan and Petrov [6] assume $H(q^2) \approx$ const ≈ 1.7 GeV^{-1}; Ali and Parkhomenko relate $H(q^2)$ to the expansion of the two light-cone distribution amplitudes (LCDA) describing the quark and gluon components of the η' wave function [14]. Figure 7 shows the measured dn/dZ distribution, compared with three representative choices for $H(q^2)$: $H(q^2) = H_0 = 1.7$ GeV^{-1}, $H_{\rm as}$, based on the asymptotic form of the η' meson LCDAs, and $H(q^2)$ corresponding to the Ali and Parkhomenko [14] formalism, with the parameters extracted from the previous CLEO II data and the constraints from the $\eta' - \gamma$ transitions [11]. Note that in the range where $\Upsilon(1S) \to ggg^\star$ is the relevant source of η' most of the discrepancy between theory and data occurs in the $Z = 0.7$ bin. In fact, the χ^2 for the fit of the new data with this theoretical parametrization is 27 for 3 degrees of freedom. This may imply that higher order terms in the QCD expansion need to be taken into account, or that the $\Upsilon(1S) \to ggg^\star$ is not the dominant source of η', at least at a scaled energy as high as $Z = 0.7$.

In conclusion we have measured the energy spectra of the η' meson in the decay $\Upsilon(1S) \to \eta' X$. Our results are not very well described by existing models based on strong gluonic coupling of the η'. Thus the observed $B \to \eta' X$ inclusive branching fraction is unlikely to be explained by an enhanced $g^\star g \eta'$ form factor, and an explanation outside the realm of the Standard Model or an improved understanding of non-perturbative QCD effects may be needed to account for this large rate.

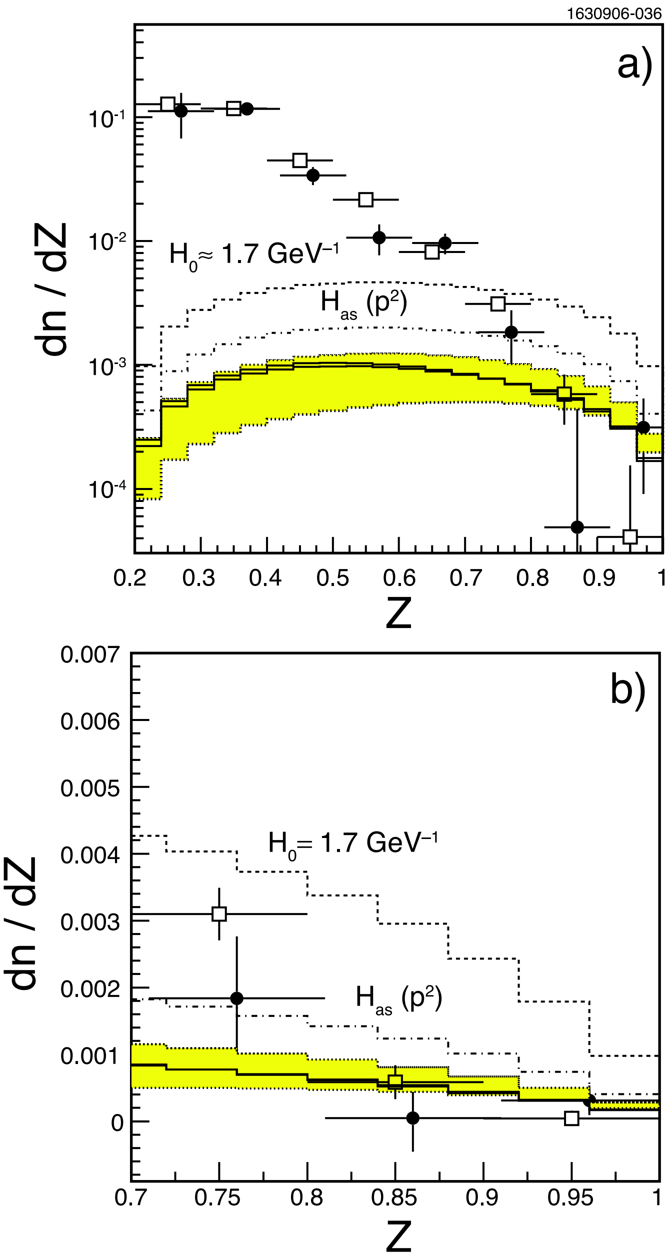

FIG. 7: Energy spectrum of the η'-meson in the decay $\Upsilon(1S) \to \eta' X$ (open squares correspond to the data presented in this paper, filled circles are the previously reported CLEO II data [13]): a) measured spectra (log scale); b) expanded view of the $Z \geq 0.7$ region to show the comparison with the theoretical predictions more clearly (linear scale). The dashed curve corresponds to a constant value of the function $H(p^2) = H_0 \simeq 1.7$ GeV^{-1}, and the dash-dotted curve ($H_{\rm as}(p^2)$) corresponds to the asymptotic form of the η'-meson LCDA [14] (i.e., $B_2^{(q)} = 0$ and $B_2^{(g)} = 0$). The spectrum with the Gegenbauer coefficients [14] in the combined best-fit range of these parameters is shown in the shaded region. The solid curve corresponds to the best-fit values of the parameters in the form factors from Ref. [14] from the analysis of the $\Upsilon(1S) \to \eta' X$ CLEO II data alone.

IV. ACKNOWLEDGEMENTS

We would like to thank A. Kagan and A. Ali for useful discussions and for providing us with their calculations. We gratefully acknowledge the effort of the CESR staff in providing us with excellent luminosity and running conditions. D. Cronin-Hennessy and A. Ryd thank the A.P. Sloan Foundation. This work was supported by the National Science Foundation, the U.S. Department of Energy, and the Natural Sciences and Engineering Research Council of Canada.

---

[1] T. E. Browder *et al.* [CLEO Collaboration], Phys. Rev. Lett. **81**, 1786 (1998) [hep-ex/9804018].

[2] G. Bonvicini *et al.* [CLEO Collaboration], Phys. Rev. D **68**, 011101 (2003) [hep-ex/0303009].

[3] B. Aubert *et al.* [BABAR Collaboration], Phys. Rev. Lett. **93**, 061801 (2004) [hep-ex/0401006].

[4] A. Datta, X. G. He, S. Pakvasa, Phys. Lett. B **419**, 369 (1998) [hep-ph/9707259].

[5] A. Kagan and A. A. Petrov [hep-ph/9707354].

[6] A. L. Kagan, AIP Conf. Proc. **618**, 310 (2002) [hep-ph/0201313].

[7] D. Atwood and A. Soni, Phys. Lett. B **405**, 150 (1997) [hep-ph/9704357].

[8] A. Ali and A. Y. Parkhomenko, Phys. Rev. D **65**, 074020 (2002) [hep-ph/0012212].

[9] W. S. Hou and B. Tseng, Phys. Rev. Lett. **80**, 434 (1998) [hep-ph/9705304].

[10] T. Muta and M. Z. Yang, Phys. Rev. D **61**, 054007 (2000) [hep-ph/9909484].

[11] P. Kroll and K. Passek-Kumericki, Phys. Rev. D **67**, 054017 (2003) [hep-ph/0210045].

[12] H. Albrecht *et al.* [ARGUS Collaboration], Z. Phys. C **58**, 199 (1993).

[13] M. Artuso *et al.* [CLEO Collaboration], Phys. Rev. D **67**, 052003 (2003).

[14] A. Ali and A. Y. Parkhomenko, Eur. Phys. J. C **30**, 183 (2003) [hep-ph/0304278].

[15] D. Peterson *et al.*, Nucl. Instrum. Meth. A **478**, 142 (2002).

[16] Y. Kubota *et al.*, Nucl. Instrum. Meth. A **320**, 66 (1992).

[17] M. Artuso *et al.*, Nucl. Instrum. Meth. A **502**, 91 (2003) [hep-ex/0209009].

[18] R. Ammar *et al.* [CLEO Collaboration], Phys. Rev. D **57**, 1350 (1998) [hep-ex/9707018].

[19] W. M. Yao et al., Journal of Physics G **33**, 1 (2006).

[20] R. Brun *et al.*, computer code GEANT3.21, CERN Program Library Long Write Up W5013 (1992).

[21] R. Kleiss and S. van der Marck, Nucl. Phys. B **342**, 61 (1990).